Efficiency of water repellent surface treatment: Experiments on low performance concrete and numerical investigation with pore network model

K. Namoulniara, P-Y. Mahieux, J. Lux, A. Aït-Mokhtar, Ph. Turcry

Efficiency of water repellent surface treatment: Experiments on low performance concrete and numerical investigation with pore network model

K. Namoulniara, P-Y. Mahieux*, J. Lux, A. Aït-Mokhtar, Ph. Turcry

Université de La Rochelle, LaSIE UMR CNRS 7356, Avenue Michel Crépeau, 17042 La Rochelle, France

* Corresponding author: pierre-yves.mahieux@univ-lr.fr

Abstract

Indicators of durability are nowadays key-parameters in the design of reinforced concrete structures. One way to guarantee durability is usually to design concrete mixtures with low porosity and low transfer properties. An alternative or in addition to this performance-based approach is the use of treatments such as water repellent, applied on surface of both new and existing concrete structures. The aim of the present study is to evaluate the efficiency of two water repellents with respect to water capillary absorption. Both studied water repellents were applied on a concrete with relatively low mechanical performances (28-day compressive strength equal to 20 MPa). Porosity, pore structure and capillary absorption kinetics were determined according to the AFREM recommendations [Arliguie et al., 2008] for both treated and non-treated concrete samples. The water repellents were found to significantly reduce the water absorption kinetics. However, this reduction was shown to be temporary. The surface treatments slow down the water transfer but when the water passes through the physical barrier, the kinetics capillary absorption becomes similar to that of non-treated concrete. A pore network model was used to support this explanation of the observed absorption kinetics and to model the effect of water-repellent.

1 Introduction

Corrosion due to aggressive agents such as chloride is the most frequent pathology of reinforced concrete structures [Costa, 2002], [Poupard et al., 2003]. Corroded structures need expensive repairs. Ollivier et al. pointed out that the United States of America should dedicate a budget of more than $ 100 billion during ten years for repairs [Ollivier et al., 2008]. The use of mortar patches is a common method to repair of corroded structures [Canisius, 2004], [Soufi et al., 2016]. Alternative solution to avoid spending time and money in maintenance is to protect newly cast concrete structures with surface treatments, which limit the diffusion of aggressive agents through the concrete cover. The European standard EN 1504 defines three types of surface treatments [EN 1504, 2005]: coatings, impregnations and hydrophobic impregnations. Coatings produce a hydrophobic layer on the exposed concrete surface. Impregnations reduce the cover porosity by filling partially or completely capillary pores. Hydrophobic impregnations, also called water repellent agents, are surface treatments designed to protect concrete against water penetration. Their chemical components reduce surface tension and turn concrete into a hydrophobic material. Unlike coatings, no film forms on the cover surface and the concrete appearance remains unchanged: only the surfaces of capillary pores are coated with the hydrophobic substances.

Since the 1970's, many researches were conducted to evaluate the performance of repair products. Basheer et al. give an overview of the scientific studies conducted on the methods of assessment and performance of surface treatments [Basheer et al., 1997]. More recently, other works complete this literature review [Schueremans et al., 2007], [Medeiros, 2008 and 2009], [Pigino et al., 2012], [Pan et al., 2017]. Surface treatments tend to improve the performance of concrete against the penetration of aggressive agents and service-life of concrete structures. Johansson shows that the penetration of chloride ions is reduced from 70% to 80% [Johansson, 2006]. Medeiros shows that the diffusion coefficient of chloride is reduced by 80%, while the capillary absorption coefficient is reduced from 73% to 98% [Medeiros, 2008]. Zhao et al. confirm that the dissolved ions cannot penetrate the porous network because the water penetrates only in vapor form [Zhao et al., 2005]. Basheer et al. state that it is important to study the behavior of concrete treated in their environment and also for a long term period because it seems that the water

repellents are sensitive to climate conditions (UV attacks, freeze-thaw cycles, etc.) and their ability to protect the concrete can be reduced [Basheer et al., 1997]. However, Schueremans et al. [Schueremans et al., 2007] show, through a study focused on the quality and quantity of water repellent agents, that it is possible to obtain good results in the long term with respect to the penetration of aggressive agents and thus in protection of reinforced concrete structures.

Putting aside the eventual degradation of water repellents, many studies agree that these protections are effective for reducing the transfer process and particularly the water absorption. One can, however, wonder how long the protective effects last, since only a small depth of the cover is usually impregnated by the hydrophobic treatment. Thus, one can wonder if protection remains efficient when aggressive agents have diffused beyond the treated depth.

In order to answer this question, the long term efficiency of two standard water repellent agents were investigated in the present study. An experimental campaign was carried out on a concrete with poor mechanical performances. This kind of concrete was chosen in order to reduce the time of the mass transfer phenomenon investigated in our laboratory work, namely water capillary absorption. Microstructure of treated and non-treated concrete specimens was also investigated. In parallel, numerical simulations based on a pore network model were also carried out in order to complete our investigation on the effects of the porous network connectivity reduction and the penetration depth on the capillary absorption.

2 Materials and experimental procedures

2.1 Water repellents

Two water repellents agents were studied: the first agent (denoted H1) is composed of siloxanes molecules, while the second one (denoted H2) is composed of silanes molecules.

Silanes are a family of monomers molecules derived from different alkyl groups linked to each other by a silicone molecule (Figure 1). The waterproofing properties of silanes come from a double chemical reaction (hydrolysis and condensation) between water repellent and concrete. Silanes molecules react with the interstitial water to form silanols groups (reaction in an alkaline solution at high pH value) and ethanol. Silanols groups then react with siliceous phases (aggregates and cementitious matrix) to form a hydrophobic layer on the surface of concrete pores (alkyl group). Generally, larger the molecule of the alkyl group is, better the repellency of the silane is. Silanes are volatile and some active components can evaporate during the application, especially if the operation does not take place under ideal conditions.

Siloxanes are oligomer molecules derived from partially hydrolyzed molecules of silanes. Siloxanes react with concrete silica to form a hydrophobic layer. In concrete pores, the reactions are identical to those described for the silane molecules, with a residual hydrolysis and polycondensation.

Figure 1: Silane and siloxane molecule [Johansson, 2010]

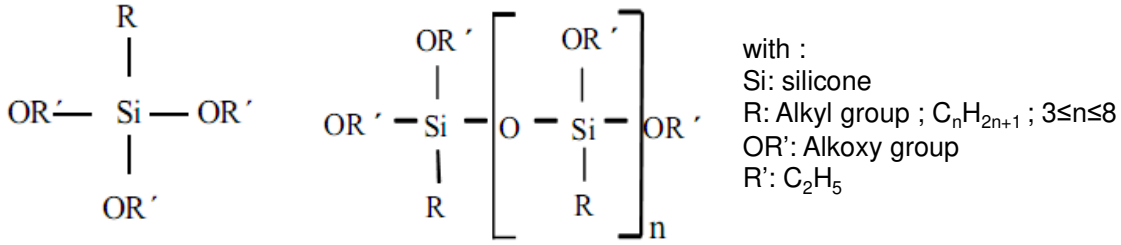

Silane molecule Siloxane molecule

Water repellents were applied on the surface of the tested specimens (described in the following section) by paintbrush in two coats for an overall quantity equal to 300 g/m^2 (i.e. at 150 g/m^2/coat). To ensure a complete polymerization, the treated specimens were conserved 14 days in room conditions before furthers investigations.

2.2 Concrete

Experiments were carried out on a low performance concrete made with a Portland limestone cement CEMII/B-LL/32.5, with a 0/4 mm siliceous sand and a 6/10 mm diorite coarse aggregates. Concrete composition, given in table 1, has been investigated in previous research program [Tahlaïti, 2010], [Soufi et al., 2016]. Due to its high W/C ratio, this concrete has a relatively high porosity (table 2) and low mechanical performance (compressive strength equal to 20 MPa at 28 days), what makes it convenient for accelerating mass transfers and highlights in a reasonable time the impact of water repellent agents used.

Table 1: composition of studied concrete (per cubic meter)

Constituents	Mass (kg)
Portland limestone cement	275
Water	222
W/C	0.8
Fine aggregates 0/4	729
Coarse aggregates 6/10	1085

Concrete cylinders (Φ11x22 cm) were cast, demoulded at 1 day and conserved in water at 20°C during 21 days. After this curing period, some cylinders were cored and sawn to obtain slices with 65 mm in diameter and 30 mm in height. These specimens were used for porosity and water repellent penetration depths measurements. A second series of cylinders was sawn to obtain cylindrical specimens with 110 mm in diameter and 50 mm in height. The latter were used for capillary absorption tests. All the specimens were placed after sawing in a room at 75±5% RH and 20°C during 7 days. This conservation was required to have sufficiently dry surfaces before the application n of water repellent.

Among all the specimens, some of them (denoted C15) were non-treated and used as reference, others were treated with the water repellent H1 and H2 (denoted C15H1 and C15H2, respectively). Note that the water repellents were applied only on one sawn surface of the specimens (i.e. one plane circular surface). The experimental program is summarized in Figure 2.

Figure 2: Summary diagram of the experimental procedure

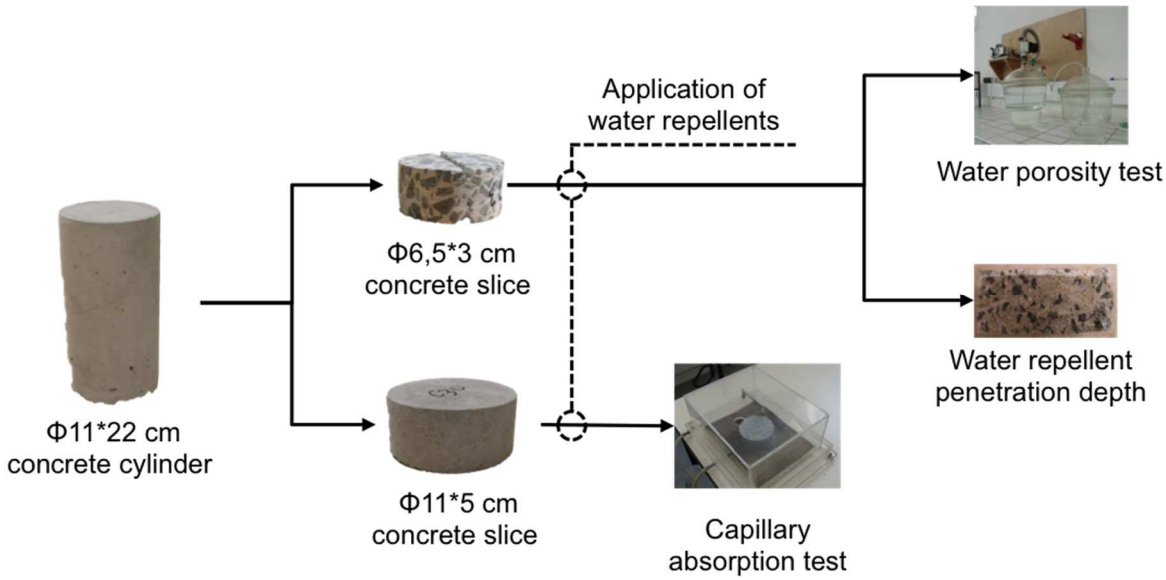

2.3 Experimental procedures

To measure the penetration depths of the water repellents, the 30 mm thick slices were split into two parts then split areas were sprayed with water, according to the European standard [EN 1504, 2005]. The penetration depths were measured with a ruler and correspond to the thickness remained dry due to the hydrophobic effect of water repellent.

The water porosities were assessed according to the French standard NF P 18-459 [NF P 18-459, 2010]. Specimens were water-saturated during 24 hours under vacuum (around 2.5 kPa) and then oven-dried at 105°C. Volumes were determined by hydrostatic weighing. The average of water porosities values were calculated form three results for each study case.

Mercury intrusion porosimetry (MIP) was carried out with the Micrometrics Autopore III 9420 porosimeter, according to a procedure recommended by the AFPC-AFREM [Arliguie et al., 2008]. The test was performed on 15 mm side cubes sawn from the 30 mm thick slices. In the case of treated slices, these cubic samples contained the treated zone (determined previously with the penetration depth). Before mercury intrusion, the cubic samples were dried during 7 days at 45°C in a ventilated oven.

Capillary water absorption tests were performed following the procedure proposed by the AFPC-AFREM [Arliguie et al., 2008]. The lateral faces of the 50 mm thick specimens were sealed with a resin coating to insure unidirectional transport from bottom to the top during absorption. Before testing, specimens were dried at 80°C

until weight stabilization. They were cooled and then put in contact with water (Figure 2). Specimens were regularly weighted during the test.

A FEI/Philips Quanta 200 SEM was used to make images on non-polished layer samples in environmental conditions, in order to locate the water repellents and observe their microstructures.

3 Experimental results

3.1 Penetration depths

As shown in Figure 3, the average penetration depth of C15H1 is lower than the penetration depth of C15H2, with 2.5 and 9.5 mm average depths, respectively.

When applied on a concrete surface, the water repellent goes into the cement matrix by capillary suction. This absorption follows the classical Washburn law [Aït-Mokhtar et al., 2004] during 6 to 8 hours according to Gerdes et al. [Gerdes et al., 2001]. After that, the absorption slows down due to chemical reactions taking place in the porous network (hydrolysis and polycondensation, see section 2.1). Over time, these chemical reactions and the consecutive condensation prevent any additional penetration of water repellent.

The absorption of a water repellent depends, on the one hand, on the chemical nature (type of cement, nature of aggregates, temperature, pH), the physical properties (i.e. porosity) and the water saturation degree of the concrete substrate, and, on the other hand, on the application, the quantity and the quality of the water repellent agent. In this study, the main reason that can explain the difference between the penetration depths is the molecular structure of the studied products and the chemical reactions that occur during the absorption phase, since all other parameters remain constant.

The water repellent H1 is a siloxane solution in solvant phase. The siloxane molecule is itself a silane molecule partially hydrolyzed. When siloxane contacts the interstitial solution, a residual hydrolysis takes place very quickly causing the formation of polysiloxanes. These polymers create a hydrophobic barrier that reduces and even cancels the additional absorption of the product, which explains the lower penetration depth of H1. This assumption seems to be confirmed by SEM analyses. A thin film can be seen on the concrete surface (image 3, Figure 3) revealing the presence of

H1 repellent on the surface, while no film can be detected on the surface of the sample treated by H2 (image 4, Figure 3).

The water repellent H2 is a pure silane solution (99 % of actives substances). The time required for complete hydrolysis and poly-condensation is longer than that of H1. Furthermore, the smaller size of the H2 molecules allows the water repellent to penetrate the pores network inaccessible to the H1 siloxane molecules. The combination of these two parameters allows the H2 water repellent having a better penetration depth in comparison with H1.

In addition, images 5 and 6 in Figure 3 show that microstructures of water repellents after condensation are identical in both cases with agglomerated forms, partially distributed on the pores surface.

Figure 3: Multi-scan approach of water repellents penetration (image 1 and 2: transversal sections, images 3 and 4: SEM scans of concretes surface, images 5 and 6: SEM scans of the pores surface

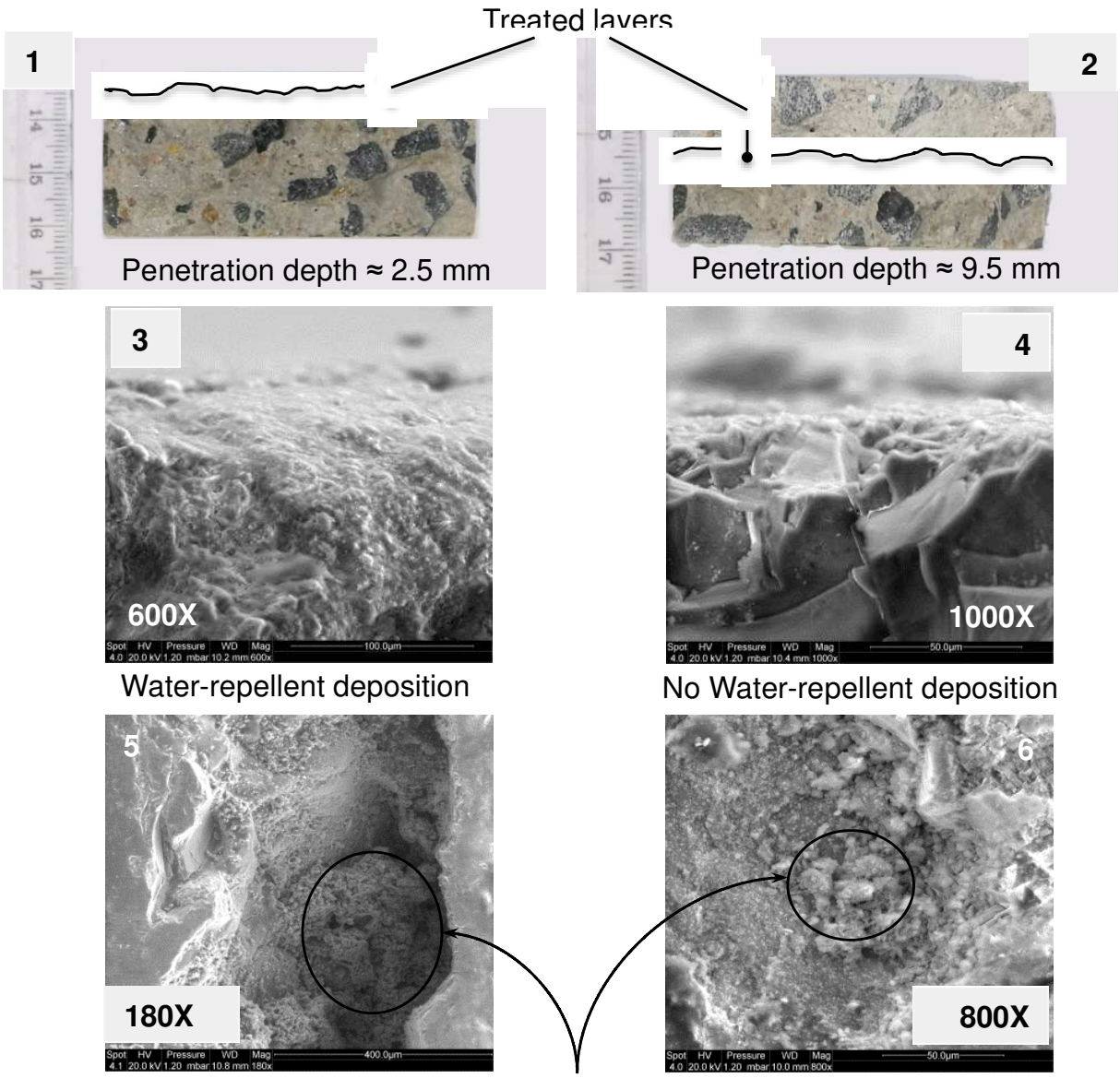

3.2 Water porosities

Table 2 gives penetration depths and water porosities obtained on the reference concrete C15, C15H1 and C15H2. Note that C15H1 and C15H2 samples are composed both of treated concrete and non-treated concrete layers, since the penetration depths are less than the smallest dimension of samples (30 mm).

Table 2: Measured penetration depths of water-repellent and water porosities of C15, C15H1 and C15H2

	Penetration depth (mm)	Water porosity (%)
C15	0	14.9 ± 0.5
C15H1	2.5 ± 0.5	13.2 ± 0.1
C15H2	9.5 ± 2.5	8.1 ± 0.5

The reference C15 concrete has the highest water porosity with 14,9%. As planned, with this high value, this concrete can be classified under the low durability category structure materials [AFGC, 2004]. The lowest porosities were determined on C15H1 and C15H2 concretes with 13,2% and 8,1%, respectively. Note that porosities of the treated specimens are inversely proportional to the penetration depth of water repellents. In view of these results, we can question the effectiveness of this method. Indeed, if we use the measured water porosities in the two treated samples as a basis for calculating the porosity in the treated layer, we found negative values, even when taking into account the measurement uncertainties. This can be explained by two things: first, it is possible that zones that are only partially filled by water repellent could not be detected visually. The boundary between the treated and untreated zone is probably more gradual than what is observed on the photographs. Secondly, it is likely that water will not be able to enter the porous network partially or totally treated with a water repellent, despite the vacuum imposed in the desiccator. The saturation time imposed during 24 hours was not sufficient to obtain a complete saturation of the treated layer.

Although the treated layers have a hydrophobic behavior, the problem encountered in the determination of the water porosity can also be related to the reduction of the pores connectivity. Water repellent cover partially or totally the pore surfaces. This behavior occurs when the size of polymerized water repellent molecule is lower than

the pores diameter. The siloxane molecular structure is close to polymerized molecule. We can assume that the pores diameter ranging from 3 to 30 nm (the size of siloxane molecules) in the case of C15H1 and between 0.4 and 30 nm in the case of C15H2 are no longer accessible to water. This hypothesis is confirmed by MIP curves shown in Figure 4. For the pore size distribution range from 5 to 19 nm and 3 to 19 nm respectively for the C15H1 and C15H2, the volume of mercury that has penetrated the sample is really smaller than in the case of the reference concrete.

Figure 4: Pores size distribution of C15, C15H1 and C15H2 concretes

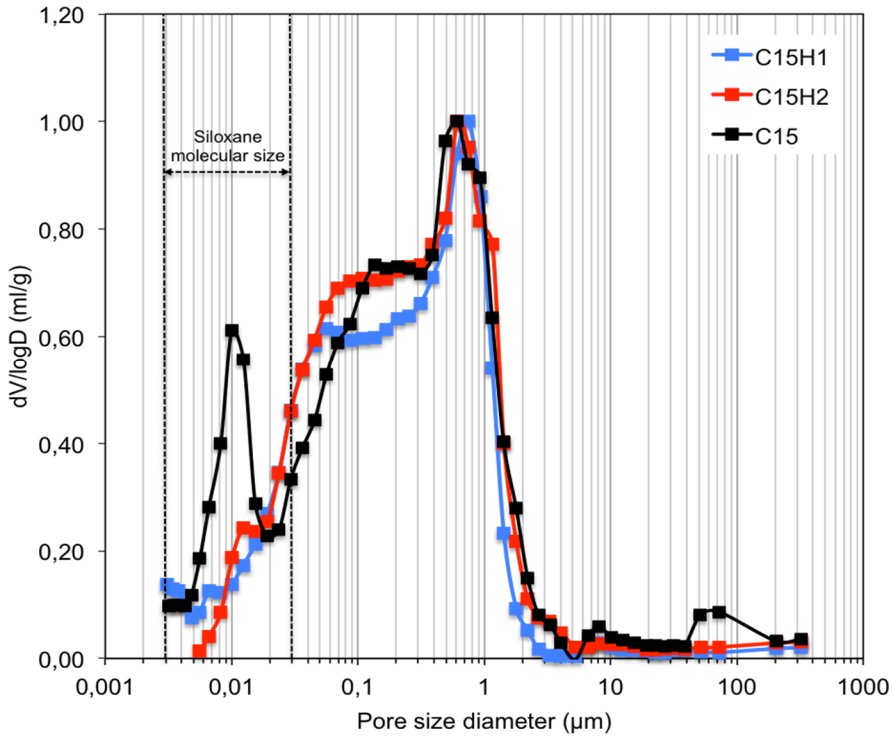

Finally, it seems that the treated layers can be only very partially water-saturated. However, as shown in the following section, the water-absorption is sufficient to ensure a percolation through the treated layer.

3.3 Capillary water-absorption

Figure 5 gives the time-evolution of the specimen mass during the absorption test. The non-treated specimen has a classic kinetic of capillary absorption [Ollivier et al., 2008], with a linear evolution of the absorbed water mass per unit volume in function of the square root of time until saturation. This law does not apply to the water repellent concretes, particularly during the first four hours of capillary absorption, where the amount of absorbed water is lower than the one observed for the

reference concrete. Capillary absorption curves of the treated concretes can be divided into three parts, as follows:

Phase I: when the treated concrete sample is placed on capillary absorption test, water does not immediately penetrate the porous network because the external surface is hydrophobic, as shown by the capillary contact angle test (Figure 6). In both cases, the initial contact angle is clearly greater than 90°, revealing a low wetting surface, with 92° and 122° respectively for the C15H1 and C15H2. However, on the surface of treated samples, the hydrophobic effect is temporary, since the contact angle is not constant with time: it decreases quickly. In the best case, it takes up to 45 minutes for a drop of water to completely penetrate the material. In fact, the water repellent does not prevent the water vapor diffusion [Johansson et al., 2009] [EN 1504, 2005]. Under a moisture gradient, the water molecules will be adsorbed on the internal surface of the concrete pores and on the water repellent alkyl groups. Over time, it creates a continuous water film, which gradually reduces the effect of the water repellent and consequently increases capillary absorption.

This phenomenon is observed in both cases and corresponds to the significant change in the slope of the absorption curves. This change indicates the time required for the continuous film to form and it is sufficient to create a percolation through the untreated material. For the C15H1 and C15H2, it occurs after 45 minutes and 4 hours, respectively. This second water repellent H2 protects much longer than the H1, although these two products only protects very temporarily. This latest observation is very remarkable and highlights the limit of these two water repellents for the protection of concrete structures. In addition, the required amount of water to ensure a percolation is similar in both cases, i.e. about 10 kg/m^3. This means that the water fills about 1% of the overall porosity. It is unlikely that this amount of water will fill the entire the porous network of the treated layer.

Phase II: The capillary absorption curves follow a conventional kinetics (similar to the reference concrete), indicating that water is in the untreated layer. However, the absorption kinetics are still lower. The repellent layer provides greater hydraulic resistivity thereby reducing the overall conductivity of the treated samples. This effect is greater when the depth of penetration increases (i.e. for C15H2).

Phase III: This phase corresponds to the moment when the water reaches the upper face of the sample. Unlike the C15, C15H1 and C15H2 need about respectively 24 hours and 4 days to reach their maximum absorption. In the case of C15H1, the

amount of absorbed water is the same as the C15. The thin penetration depth of this water repellent is insufficient to observe a significant decrease of the total amount of water absorbed. However, we notice a significant decrease of water absorbed in the C15H2 sample.

Therefore, the water repellent increases the time required to reach the maximum absorption but not enough to protect over time the concrete structures against the aggressive agents. These results show that the effectiveness of water repellents depends mainly on the depth of penetration.

Figure 5: Capillary absorption of C15, C15H1 and C15H2 concretes

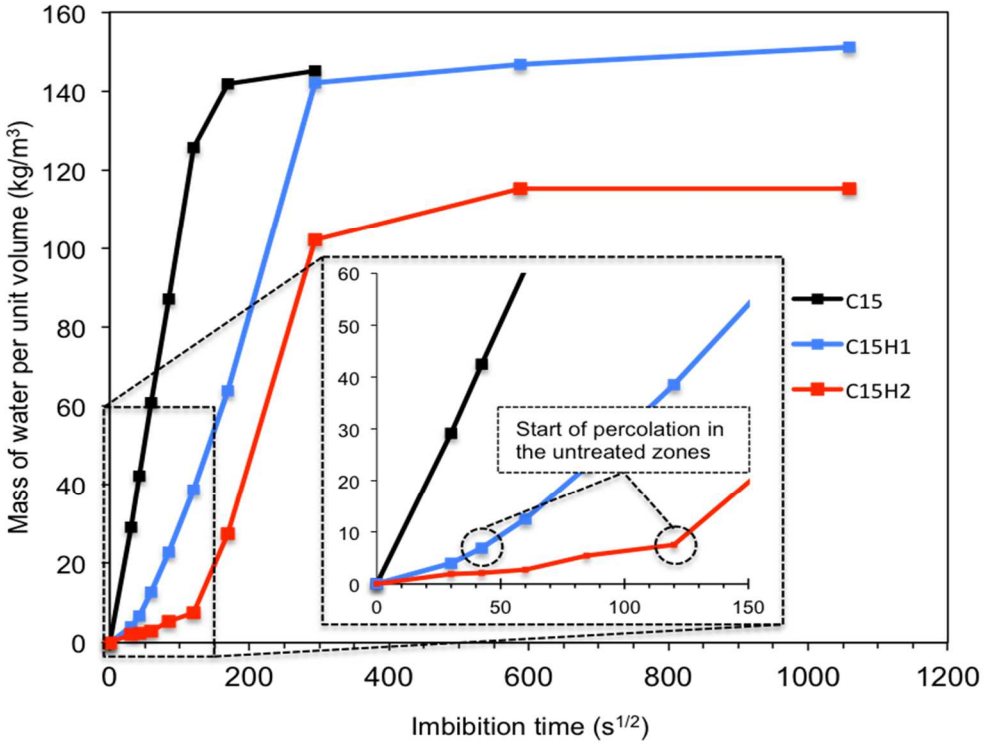

Figure 6: Contact angle as a function of time and water repellents used (H1 and H2) on C15 concrete

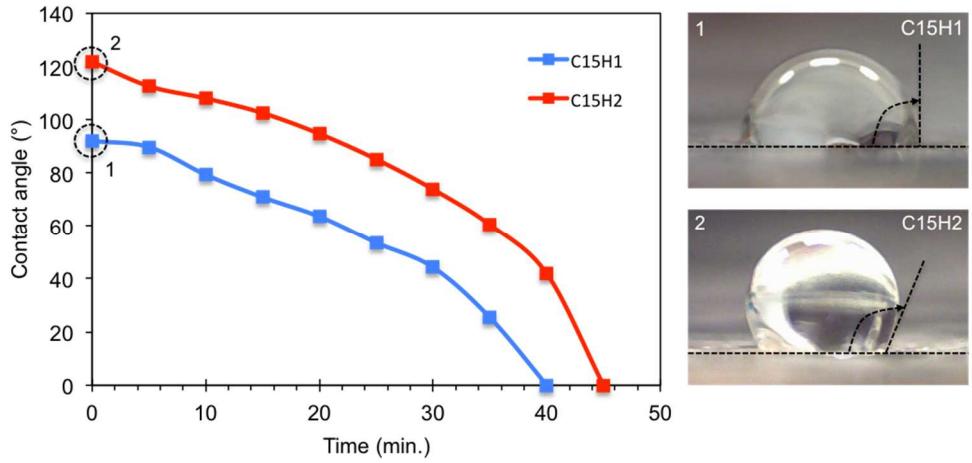

These results do not challenge the quality of the water repellents used, but rather their effectiveness to protect over time the concrete structures against the capillary absorption. In the literature, researchers focused their studies on concretes specially formulated for aggressive environments and have not highlighted this phenomenon. All are unanimous to say that these surface treatments have a real effect on the absorption and hence are effective to limit the transport of aggressive agents but none of them quantify the temporary effect of this maintenance system. For a predictive approach to sustainability maintenance by surface treatments, our results highlight the necessity to extend existing studies since it seems that this phenomenon observed on a low-quality concrete is also valid on all types of concrete.

4 Modeling of capillary absorption

In order to complete the experimental study, numerical simulations of capillary absorption using a pore network approach were carried out. This numerical approach aims at simulating the effects of the porous network connectivity reduction and the penetration depth on the capillary absorption.

4.1 Modeling principle

Pore network models were used successfully to study a wide range of multiphase flows and to predict effective properties like permeability [Amiri et al., 2005]. In this work, we use a dynamic pore network model derived from generic “ball-and-stick” models [Blunt et al., 1992], [Leventis et al., 2000], [Valavanides, 2001], [Gielen, 2007]

within which pore bodies and throats are represented by spheres and straight cylinders with circular cross-sections, respectively. These models only allow “piston type” motion, in which the invading wetting fluid advances in a connected front that occupies the bulk of the pore space. A detailed description of the model is available in [Lux & Anguy, 2012].

We consider 3D networks made of pores arranged on a regular cubic lattice and connected by throats. In this kind of networks, the coordination number (i.e. the number of throats connected to each pore) is 6.

4.2 Construction of pore networks

The pore size distribution for the reference network, which represents the untreated sample, is partially based on the MIP results. The objective here is not to create a realistic pore network, which is a quite difficult task (see for instance [Tsakiroglou, 2000]), but to create a network with a correct range of pore sizes. We use two Gaussian distributions noted G1 and G2 in order to generate two distinct populations of pores. Table 3 summarizes the properties of the chosen distributions and their respective probability, as well as the prescribed minimum and maximum radii. The radius R_{ij} of a throat connecting two pores i and j of radii R_i and R_j respectively, is uniformly distributed between $\min(R_i,R_j)$ and $\min(R_i,R_j)/2$. Figure 7a and 7b show the pore and throat radius distributions measured on a realization of a pore network made of 10x25x10 pores along x, y and z-axes, respectively.

Table 3: Pore size distributions for the reference network

	Average radius (nm)	Standard deviation (nm)	Probability	Minimum radius	Maximum radius
G1	400	100	40%	1	1000
G2	10	5	60%	1	100

Figure 7: Pore radius distribution (a) and throat radius distribution (b)

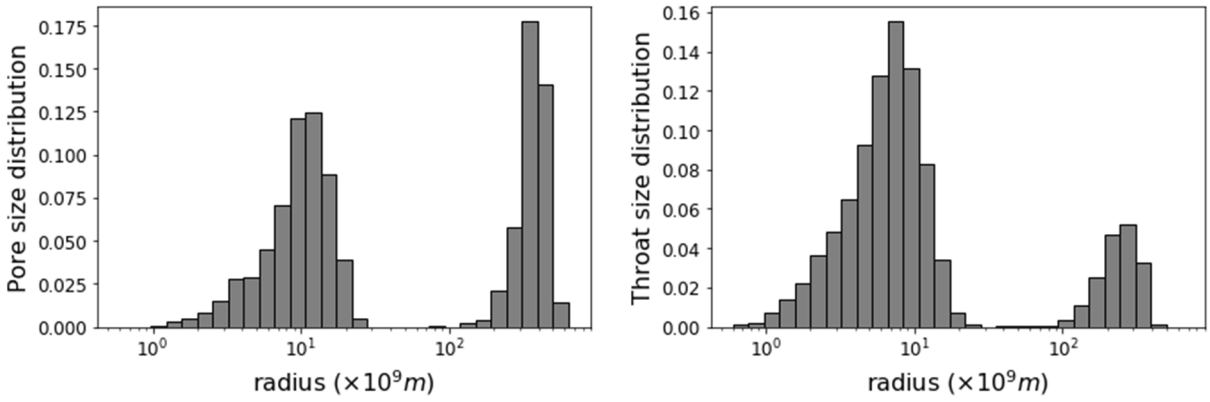

(a) (b)

As shown in the previous section, the porosity of the concrete sample is reduced in the layer where the water repellent penetrates. The MIP curves show that the proportion of small pores is reduced in the treated samples. As said previously, it is likely that the smallest pores are entirely filled by the water repellent, what reduces the connectivity of the pore network and hence the porosity. If the water repellent enters other pores, there is no evidence that it modifies notably their radius.

In this work, we consider that water repellent enters preferentially into the smallest pores and fills them entirely. We use a simple invasion percolation algorithm is used in order to simulate the penetration of the water repellent into the network and the subsequent reduction of the porosity (Ferer et al., 2003). This algorithm works as follows: the smallest pore located at the bottom surface is first marked as filled. Then, at each iteration, the algorithm looks at all neighbors of the currently filled pores and immediately fills the smallest of all the neighbors. As filled pores are non accessible to water, they are therefore deleted from the network. The algorithm stops when the porosity of the layer is lower or equal to the porosity objective, which is arbitrarily set to 1/3 of the initial network porosity. Note that connectivity checks are performed at each iteration to ensure that the deletion (i.e. filling) of an element does not lead to the creation of two disconnected networks. Thus, all the empty pores remain connected to the whole network and to the inlet (i.e. there is always at least one path that connects two pores in the network). The porosity objective in the layer being very small (around 5%), this constraint is necessary to avoid the disconnection of all the remaining pores from the inlet.

Figure 8 shows a realization of a network made of a 10 x 25 x 10 pores and the results of our algorithm for a layer height of 30% of the total network height. Note that the connectivity in the layer partially filled by the water repellent is drastically reduced.

Figure 8: A realization of a 10 x 25 x 10 pore network before (a) and after (b) removing small pores in a layer of thickness equal to 30% of the total height of the network.

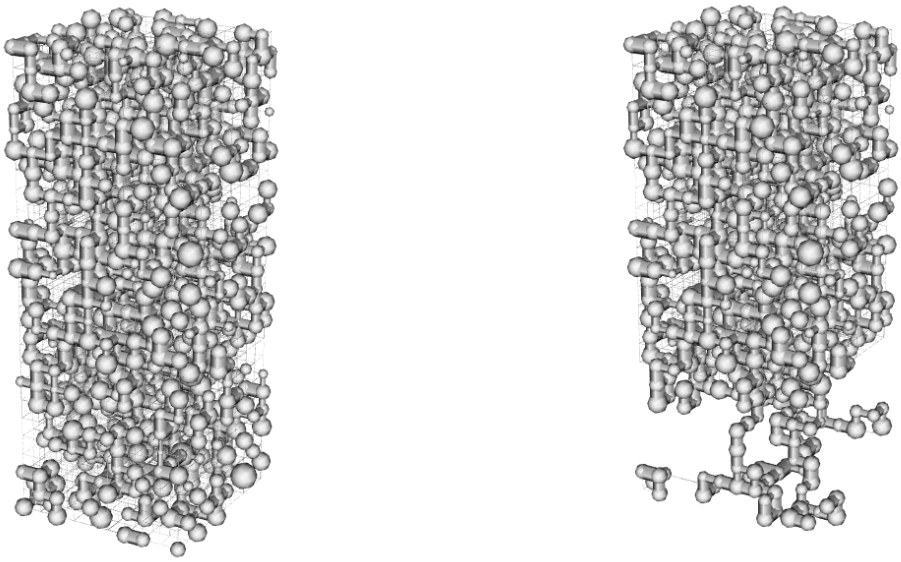

(a) (b)

4.3 Simulations of water capillary absorption

Simulations of free imbibition are carried out on several realizations of network of size 8.9 x 22 x 8.9 μm^3 made of 10 x 25 x 10 pores. In order to study the influence of the layer thickness on the imbibition kinetics, the base network is modified using the aforementioned procedure to generate layers of thickness equal to 5%, 10%, 20% and 30% of the total height of the base network. Porosity is fixed to 15% in the base network and is reduced to approximately 5% in the layer where the water repellent penetrates.

Water invades the network from the bottom (y=0), and air can escape from the opposed face (top). The other sides are impermeable to water and air. Initially, all pores are filled with air, except for the pores in contact with the water reservoir, which are half filled. The water pressure at the inlet is constant and fixed to a value close to the atmospheric pressure (100kPa) like in previous experiments, and the same applies for the air pressure at the outlet. Simulation ends when all air is trapped.

Figure 9 shows different stages of the imbibition in a realization of a pore network with a treated layer thickness equal to 20% of the sample height. Figure 10 shows the evolution of the water saturation for each network versus the square root of time. Note that the water saturation stabilizes only after a very short time. This is due to the small dimensions of the studied network. What is important here is the relative difference between all numerical experiments.

Although air trapping is more important in the numerical simulations than in the experimental results, the general behavior is very similar. In the modified part of the studied networks (treated layer), the imbibition kinetic is indeed far slower than for the reference network until the height of the water front exceeds the layer thickness. In a second part, the slope of the curves greatly increases and remains constant until the water front reaches the top of the network, which indicates that the imbibition follows a classical Washburn law. Note that the slopes of the first and second part are both smaller when the thickness of the treated layer increases.

The slow kinetic observed in the first part is the consequence of:

- The reduction of the macroscopic hydraulic conductivity in the layer, due to the lower porosity but also to the lower connectivity of the pore network.
- The reduction of the macroscopic capillary pressure, due to the fact that the layer contains far fewer small pores than in the reference network.

When the fluid enters the unmodified part of the network, i.e. the part where the water repellent has not penetrated, the capillary flow is only affected by the reduction of the hydraulic resistance in the layer, which explains that the imbibition kinetic becomes slower than in the reference network when the thickness of the hydrophobic layer increases. Note however that the flow pattern can be altered by the low connectivity in the layer. For example, Figure 8b shows a typical capillary fingering pattern, which partly explain the important trapping observed in the simulations.

Pore network simulations allow reproducing qualitatively the observed experimental behavior. It is a good indication that the observed kinetics may be partly explained by the filling of the smaller pores by the water repellent. However, one can notice that the experimental kinetics in the layer is slower than in simulations. This could be explained by other effects, which are not taken into account in the numerical simulations. In particular the contact angle is assumed to be zero and constant in simulations. Even if Figure 5 shows that the contact angle at the surface decreases quite quickly, we have no indication about the evolution of the wettability inside the

concrete sample. It is likely that the average contact angle is greater inside the treated layer than in the rest of the network, which decrease the capillary pressure inside the layer.

Figure 9: Visualization of the pore network at different stages of the imbibition: (a) water begins to fill the unmodified part of the network, (b) final state in the modified layer, (c) percolation and (d) final state.

Empty pores are colored in white while filled pores are either colored in blue or in red. Red pores are located in the layer where the water repellent penetrates, while blue pores are located in the unmodified part of the network.

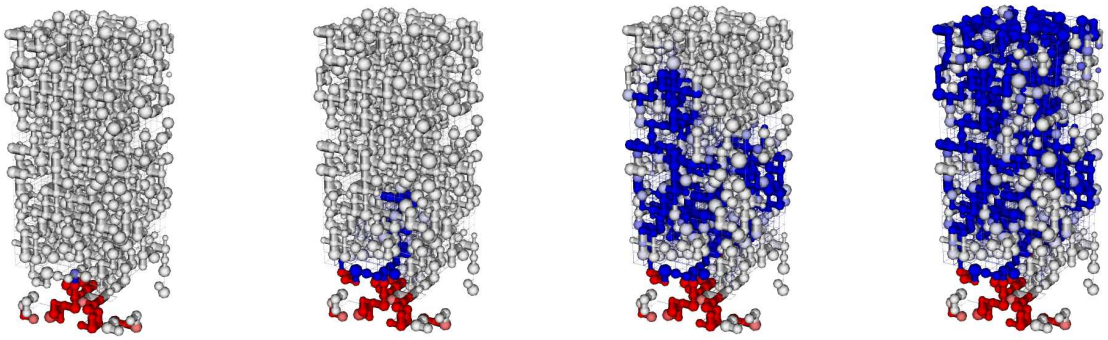

Figure 10: Imbibition kinetics for different layer thicknesses expressed in percentage of the total height.

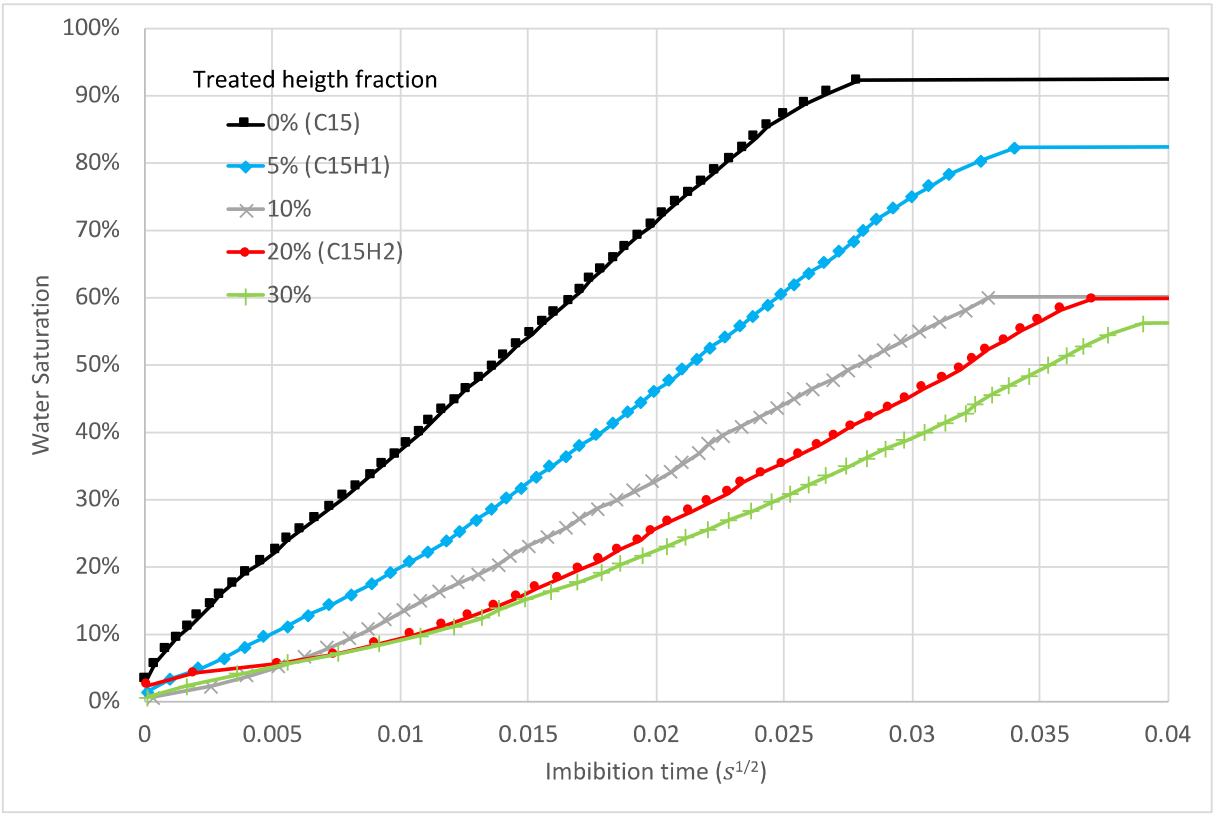

5 Conclusion

In this paper, we have studied the effects of two water repellent agents on the water imbibition kinetics and on the microstructure of a relatively low performance concrete. Numerical simulations based on a pore network approach were also carried out to support our experimental findings. Based on our results, the following conclusions can be drawn:

- The water porosity of concrete samples is reduced in the treated layer by water repellent penetration. The internal face of concrete pores is coated with the hydrophobic water repellent, which fills primarily the smallest pores and reduces consequently the connectivity of porous network. This explains why it is difficult to access the global porosity of specimens treated with water repellent.
- The efficiency of the water repellents to reduce capillary absorption kinetics depends of their penetration depth.
- The repellent effect is quite limited in time. When water exceeds the limit of the treated layer, the absorption kinetics become quite similar to those of the non-treated concrete. The capillary absorption coefficient is however lower due to a lower hydraulic conductivity in the treated layer.
- Pore network simulations allow reproducing qualitatively the experimental behavior. This supports the fact that the observed kinetics may be partly explained by the filling of the smallest pores by the water repellent.

These results confirm the importance of an exhaustive preliminary study in view to protect a reinforced concrete structure in its environment. Particular attention must be paid to the perfectibility of water repellent against the water absorption kinetics in view to improve the efficiency and durability of these systems.

6 Acknowledgements

E. Conforto, research engineer (LaSIE UMR 7356 CNRS), is acknowledged for her support in the scanning microscopy investigations.

7 References

[AFGC, 2004] working group (2004), Conception des bétons pour une durée de vie donnée des ouvrages - Indicateurs de durabilité, document scientifiques et techniques, Association Française de Génie Civil (AFGC), available on website : http://afgc.asso.fr/index.php/component/hikashop/product/9-conception-des-betons-pour-une-duree-de-vie-donnee-des-ouvrages

[Aït-Mokhtar et al., 2004] Aït-Mokhtar A., Amiri O., Dumargue P., Bouguerra A., (2004), On the applicability of Washburn law: Study of mercury and water flow properties in cement-based materials, Materials and Structures, 37(266): 107-113.

[Amiri et al., 2005] Amiri O., Aït-Mokhtar A., Sarhani M., (2005), Tri-dimensional modelling of cementitious materials permeability from polymodal pore size distribution obtained by mercury intrusion porosimetry tests, Advances in cement research, 17(1): 39-45.

[Arliguie et al., 2008] Arliguie G., Hornain H., (2008), GranDuBé, grandeurs associées à la durabilité des bétons, 1ère éd., ENPC, Paris, FRANCE.

[Basheer et al., 1997] Basheer P.A.M., Basheer L., Cleland D.J., Long A., (1997), Surface treatments for concrete: Assessment methods and reported performance, construction and building materials, 11(7-8): 413-429.

[Blunt et al., 1992] Blunt M.J., King M.J., Scher H., (1992), Simulation and theory of two-phase flow in porous media. Phys Rev A 46: 7680-7699.

[Canisius, 2004] Canisius T., Waleed N., (2004), Concrete patch repairs under propped and unpropped implementation. Proceedings of the Institution of Civil Engineers: Structures & Buildings, 157(582): 149–56.

[Costa, 2002] Costa A., Appleton J., (2002), Case studies of concrete deterioration in a marine environment in Portugal. Cement and Concrete Composites, 24: 169-179.

[EN 1504, 2005] NF EN 1504, (2005), Products and systems for the protection and repair of concrete structures, European standard, 2005.

[Ferer et al., 2003] Ferer M., Bromnhal G., Duane H., (2003), Pore-level modeling of immiscible drainage: validation in the invasion percolation and DLA limits. Phys A 319: 11-35.

[Gerdes et al., 2001] Gerdes A., Wittmann F.H., (2001), Decisive Factors for the Penetration of Silicon-Organic Compounds into surface near Zones of Concrete,

Hydrophobe III – 3rd International Conference on Surface Technology with Water Repellent Agents, Aedificatio Publishers, 111-122.

[Gielen, 2007] Gielen T., (2007), Dynamics effects in two-phase flow: a pore-scale network approach. Delft University of Technology.

[IQOA, 2010] Image Qualité des Ouvrages d'Art (2010), available on website : http://www.piles.setra.equipement.gouv.fr/, SETRA.

[Johansson, 2006] Johansson A., (2006), Impregnation of concrete structures – Transportation and fixation of moisture in water repellent treated concrete, Licentiate-thesis, TRITA-BKN Bulletin No. 84, Chair of Structural Design and Bridges, Department of Structural Engineering, Royal Institute of Technology (KTH), Stockholm, Sweden.

[Johanssonn et al., 2009] Johansson A., Janz M., Silfwerbrand J., and Trägårdh J., (2009), Protection of concrete with Water Repellent Agents - What Is Required to Achieve a Sufficent Penetretion Depth? Concrete Repair, Rehabilitation and Retrofitting, 763-768.

[Leventis et al., 2000] Leventis A., Verganelakis D., Webber J., Strange J., (2000), Capillary imbibition and pore characterisation in cement paste. Transp. Porous Media 39: 143-157.

[Lux & Anguy, 2012] Lux J., Anguy Y., (2012), A Study of the Behavior of Implicit Pressure Explicit Saturation (IMPES) Schedules for Two-phase Flow in Dynamic Pore Network Models. Transp. Porous Media 93: 203-221.

[Medeiros, 2008] Medeiros M., Helene P., (2008), Efficacity of hydrophobics agents in reducing water and chloride ion penetration in concrete, Materials and structures, 41: 59-71.

[Medeiros, 2009] Medeiros M., Helene P., (2009), Surface Treatment of reinforced concrete in marine environment: Influence on chloride diffusion coefficient and capillary water absorption. Construction and building materials, 23: 1476-1484.

[NF P 18-459, 2010] NF P 18-459, (2010), Concrete, testing hardened concrete, testing porosity and density, French standard, 2010.

[Ollivier et al., 2008] Ollivier J-P. et Vichot A. (2008), La durabilité des bétons, 2^{e} éd., Presse de l'école nationale des Ponts et Chaussées, Paris, FRANCE.

528 [Pan et al., 2017] Pan X., Shi Z., Shi C., Ling T-C., Li N., (2017), A review on surface
529 treatment for concrete – Part 1 : Types and mechanisms, Construction and building
530 materials, 132: 578-590.
531 [Pan et al., 2017] Pan X., Shi Z., Shi C., Ling T-C, N. Li, (2017), A review on surface
532 treatment for concrete – Part 2 : Performance, Construction and building materials,
533 133: 81-90.
534 [Pigino et al., 2012] Pigino B., Leemann A., Franzoni E., Lura P., Ethyl silicate for
535 surface treatment of concrete – Part II: Characteristics and performance, Cement
536 and concrete composites, 34(3): 313-321.
537 [Poupard et al., 2003] Poupard O., Aït-Mokhtar A., Dumargue P., Impedance
538 spectroscopy in reinforced concrete : experimental procedure for monitoring steel
539 corrosion - Part I: Development of the experimental device, Journal of materials
540 science, 38(13): 2845-2850.
541 [Schueremans et al., 2007] Schueremans L., Van Gemert D., Giessler S., (2007),
542 Chloride penetration in RC-structures in marine environment – long term assessment
543 of a preventive hydrophobic treatment, Construction and building materials, 21: 1238-
544 1249.
545 [Soufi et al., 2016] Soufi A., Mahieux P-Y., Aït-Mokhtar A., Amiri O., (2016), Influence
546 of polymer proportion on transfer properties of repair mortars having equivalent water
547 porosity, Materials and structures, 49(1-2): 383-398.
548 [Tahlaïti, 2010] Tahlaiti M., (2010), Etude de la pénétration des chlorures et de
549 l'amorçage de la corrosion en zone saturée et en zone de marnage. PhD thesis (in
550 French), Université de La Rochelle.
551 [Tsakiroglou, 2000] Tsakiroglou C.D., Payatakes A.C., (2000), Characterization of the
552 pore structure of reservoir rocks with the aid of serial sectioning analysis, mercury
553 porosimetry and network simulation. Adv. Water Resour. 23 : 773-789.
554 [Valavanides, 2001] Valavanides M., Payatakes A., (2001), True-to-mechanism
555 model of steady-state two-phase flow in porous media, using decomposition into
556 prototype flows. Adv. Water Resour. 24: 385-407
557 [Zhao et al., 2005] Zhao T-J., Wittmann F.H., Zhan H-Y., (2005), Water repellent
558 surface treatment in order to establish an effective chloride barrier, Hydrophobe IV,
559 4th International Conference on Water Repellent Treatement of Building Materials,
560 Edification Publisher, 105-118.